Transparent and UV-Reflective Photonic Films and Supraballs Composed of Hollow Silica Nanospheres

Yirang Lim, Seung-Heon Lee, Yan Li,* Seung-Hyun Kim, Tae Hui Kang, Yung Doug Suh, Soojin Lee, Yongjin Kim, and Gi-Ra Yi*

For an optically transparent, UV-reflective film, hollow silica nanospheres smaller than the visible wavelength ($<\lambda_{vis}$) are prepared and assembled into colloidal glasses, of which interstices are then backfilled with a polymer. The polymer refractive index is matched with the silica shell to minimize backscattering in the visible range, and the average distance between the hollow silica particles is adjusted by tuning the shell thickness to satisfy the interference resonance condition for a UV selective reflection. The resulting composite film shows a strong UV reflection as expected, but it is translucent in visible light due to non-negligible backscattering, which may be caused by large defects or fluctuation of the particle concentration. In order to avoid such backscattering, another polymer is introduced of which the refractive index is matched with the average refractive index of the hollow nanospheres. This allows an optically transparent film that selectively reflects the UV light. Furthermore, spherical aggregates of hollow silica nanospheres called "supraballs" are prepared and their average refractive index is matched with a solvent by adjusting the mixture ratio of water and ethylene glycol, which yields an optically transparent solution, selectively reflecting UV.

Excessive UV exposure can adversely affect organic materials used for display or photovoltaic devices, as well as, human skin,[1,2] which urges for the development of transparent but UV blocking materials. While several organic UV absorbers have been developed, they are unstable under prolonged UV radiation. This could lead to free radicals that could eventually decompose the organic matrix or damage human skin.[3,4] Alternatively, polymeric melanin hollow nanoparticles were recently reported as stable UV absorbers.[5] However, they are not colorless because of the inherent absorption of visible light by melanin. Traditionally, inorganic materials, such as ZnO, or TiO_2 nanoparticles[3,6] have been widely used as UV blocking materials because of their strong light scattering capability or UV absorption owing to their wide band gaps. However, these particles also strongly reflect visible light via scattering, thus appearing white color rather than transparent. In addition, nanoparticles are not preferred especially for cosmetic applications because growing evidence suggests that the nanoparticles could be hazardous to human health. Furthermore, a multilayer film, Bragg reflector, can be fabricated by repeated vapor deposition of ZrO_2 and SiO_2, which can also efficiently reflect UV,[4,7] but it has angle-dependency. By contrast, colloidal glasses or correlated amorphous colloidal structures[8–19] may show strong angle-independent UV reflection when "intraparticle" or "interparticle" backscattering resonance conditions[4,7] are matched for UV.

For photonic glasses made of core-shell particles, the form and structure factors can be decoupled by adjusting the shell thickness in the index-matched matrix.[20,21] Amorphous structure of hollow silica nanospheres assembled in a polymer matrix with the same refractive index as silica, also produced angle-independent colors in the visible range.[17,20,21] In those photonic glasses made of hollow particles, the core diameter was sufficiently small enough to produce backscattering peak from "intraparticle resonance" or form factor in the UV region and the structure factor peak appeared in the visible region, which corresponded to the "interparticle" distance ($=d \approx \lambda/2$).

In this report, to obtain both peaks from form and structure factors in the UV region, the core and overall diameters of hollow silica nanospheres were reduced to less than 100 nm and 200 nm, respectively. For optical transparency, the refractive index of the hollow silica nanoparticles is adjusted in the polymer matrix. At the end, we assembled hollow nanospheres into the micron sized spherical aggregates or "supraballs" by emulsion encapsulation and shrinkage for practical applications, such as UV-protection ingredients in cosmetics or coating solutions for display and photovoltaic devices.

For hollow silica particles, we have first core–shell polystyrene–silica particles by coating organosilica on polystyrene (PS) particles.[22,23] In order to avoid the formation

Y. Lim, S.-H. Lee, S.-H. Kim, Dr. T. H. Kang, Prof. Y. D. Suh, Prof. G.-R. Yi
School of Chemical Engineering
Sungkyunkwan University
Suwon 16419, Republic of Korea
E-mail: yigira@skku.edu
Dr. Y. Li, S. Lee, Dr. Y. Kim
Materials Research Lab
Amorepacific R&D Unit
Yongin 17074, Republic of Korea
E-mail: leeyun@amorepacific.com
Dr. Y. D. Suh
Research Center for Convergence NanoRaman Technology
Korea Research Institute of Chemical Technology (KRICT)
Daejeon 34114, Republic of Korea

The ORCID identification number(s) for the author(s) of this article can be found under https://doi.org/10.1002/ppsc.201900405.

of random aggregates by bridging during the coating process, vinyltrimethoxysilane (VTMS) was used as an organosilica precursor.[17,23] We used 120 nm polystyrene particles as the core and grew 46 nm thick VTMS shell, which was then annealed at 600 °C for 3 h to remove the polystyrene core and densify the shell producing hollow silica nanospheres. During the thermal annealing process, the particle diameter was reduced by approximately 30% so that the particles had 94 nm core diameter and 23 nm thickness.

To prepare an inverse photonic glass film, disordered colloidal films of hollow silica spheres on a glass substrate were fabricated by a simple drop-casting process and the interstices between the hollow spheres were backfilled with trimethylolpropane ethoxylate triacrylate (TMPEOTA, SK CYTEC) and a photoinitiator (Darocur 1173, SK CYTEC). Since the refractive index of TMPEOTA ($n \approx 1.46$) is similar to that of silica ($n \approx 1.45$), the light cannot distinguish between the shell and solvent, but only recognizes the cores in the film; thus, inverse photonic glass can be obtained. The distance between the cores was approximately half the UV wavelength, which corresponded to the structure factor, and the cores were much smaller than the UV wavelength, which corresponded to the form factor (**Figure 1**a). However, the fabricated UV-reflective inverse photonic glass films containing hollow silica particles are translucent in the visible region as shown in Figure 1b and the reflection spectrum of Figure 1c. We speculated that such translucency might be due to large defects or fluctuation of the particle concentration in the film, which could cause multiple scattering in visible.
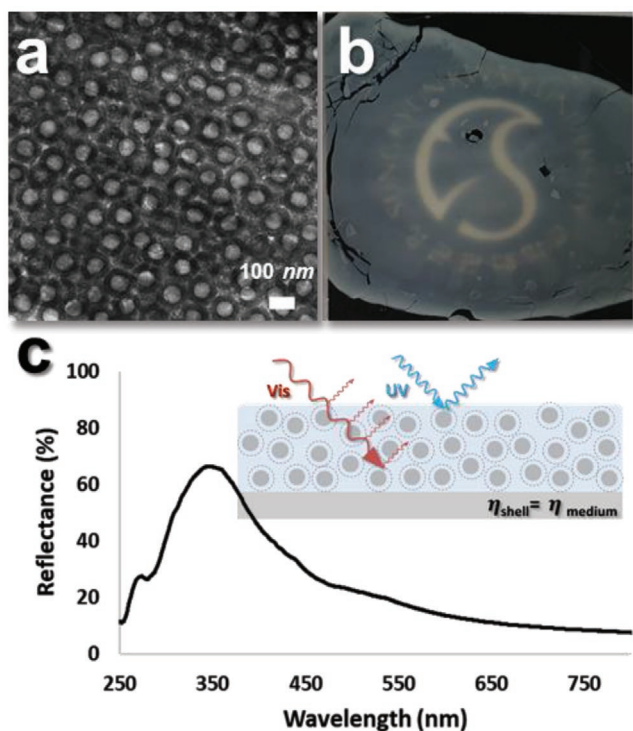

Figure 1. UV-reflective translucent inverse photonic glass films. a) TEM image and b) photograph of inverse photonic glass film of hollow silica particles in TMPEOTA matrix. c) Reflectance of inverse photonic glass film. Inset shows the schematic diagram of inverse photonic glass film.

Therefore, in order to avoid such scattering problem in composite film, the average refractive index of hollow silica nanospheres was matched to that of the matrix. As illustrated in **Figure 2**a, a dispersion of hollow silica particles in N,N-dimethylacetamide (DMAc) was mixed with poly(vinylidene fluoride-co-hexafluoropropylene) (PVDF-HFP), of which refractive index ($n \approx 1.41$) is matched with the effective refractive index of 156 nm hollow nanospheres with 76 nm cores. The effective refractive index of a hollow silica nanosphere (n_{HS}) is estimated from $n_{HS}^2 = n_s^2 f + n_{air}^2 (1 - f)$, where f is the volume fraction of the silica shell.

The mixture was simply dropped on the glass substrate and dried at 120 °C. To improve transparency, the fabricated film was thermally annealed under pressure, and the resulting PVDF-HFP film with hollow silica nanospheres showed high transmittance in the visible light, but reflectance in the UV region (Figure 2b,c). The film had an angle-independent reflectance as demonstrated in Figure S1, Supporting Information. It is noteworthy that a weak blue color from the sample was measured in the reflectance spectrum shown in Figure 2c due to a slightly broad structure-factor peak which corresponds to the relatively weak structural correlation of nanospheres or non-negligible polydispersity of interparticle distance.

Additionally, "supraballs" of hollow silica nanospheres were prepared through thermal evaporation of the emulsion droplets, where the silica nanospheres inside the emulsions were consolidated, forming disordered or quasi-crystalline structures.[13,24–30] As the inverse photonic glass films in index-matched matrix showed selective UV reflection but transparency in the visible range, we prepared supraballs of hollow silica nanospheres and dispersed them in index-matched solvent to obtain a UV-reflective solution, as shown in **Scheme 1**.

To prepare supraballs of hollow silica nanospheres, we first modified the PS-VTMS core-shell particles with hydrophobic octadecyltrimethoxysilane and then dispersed in toluene, as shown in Figure S2, Supporting Information. The colloidal suspension of the core-shell particles in toluene (10 wt%) was emulsified into a 2 wt% aqueous surfactant solution by simple mechanical homogenization (**Figure 3**a). The core-shell particles were consolidated into spherical aggregates through evaporation of toluene at 60 °C for 24 h.

As shown in Figure 3b, the average diameter of the emulsion particles was measured to be 17.8 μm with the standard deviation of 6.0 μm. After the complete evaporation of toluene, spherical aggregates of core-shell particles were obtained, which were then annealed at 600 °C for 3 h in order to remove the polystyrene cores and other organic materials in silica shell to produce supraballs of hollow silica spheres (Figure 3c). The final size distribution is plotted in Figure 3d, in which the average diameter and standard deviation were 8.2 μm and 3.5 μm, respectively. The diameter, core diameter, and shell thickness of the hollow silica spheres were 140, 94, and 23 nm, respectively. Cross sectional images of those photonic microspheres showed a clearly amorphous structure, as shown in Figure 3e, which was also confirmed by its 2D fast Fourier transformed (FFT) image (Figure 3f).[17,31]

As we demonstrated in the photonic glass films, it is important to match the average refractive index of micrometer-sized supraballs in medium for optical transparency. The effective
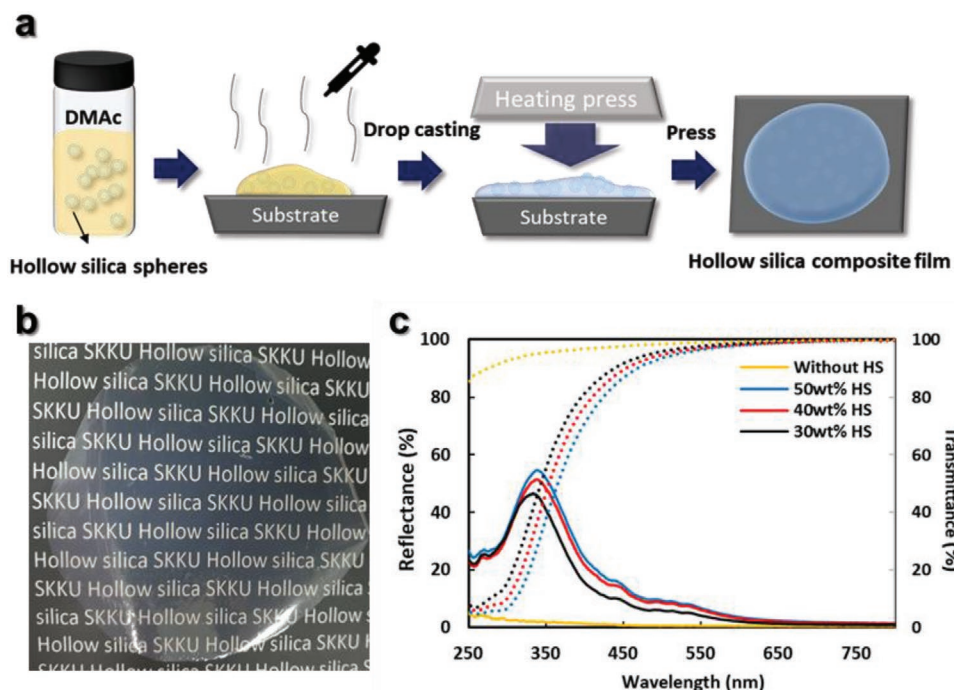
Figure 2. Visible-transparent UV-reflective photonic glass films. a) Fabrication process of composite colloidal glass films of hollow silica spheres in PVDF-HFP. b) Digital photograph of transparent and UV-reflective glass films. c) Reflectance and transmittance of composite colloidal glass films of hollow silica spheres in PVDF-HFP.

refractive index of the supraballs (n_{SB}) randomly packed with the hollow silica nanospheres is calculated using Maxwell Garnet Equation (1),

$$n_{SB} = n_m \sqrt{\frac{2n_m^2 + n_{HS}^2 + 2\phi\left(n_{HS}^2 - n_m^2\right)}{2n_m^2 + n_{HS}^2 - \phi\left(n_{HS}^2 - n_m^2\right)}} \qquad (1)$$

where n_m is the refractive index of the the medium (or solvent) and ϕ is the packing fraction.[32] Average refractive index of a

Scheme 1. Schematic illustration of transparent supraballs reflecting UV light in solvent.

hollow silica nanosphere (n_{HS}) was estimated as we described before.

The packing fraction (ϕ) of hollow silica nanospheres can be estimated by comparing the diameter of the first ring in the FFT image of the cross sectional TEM image and the first peak in the structure factor calculated using Ornstein–Zernike equation with Percus–Yevick closure approximation.[32] From the FFT images, the radius of the first ring was measured as 52.4 μm⁻¹, which is matched with the first peak of the calculated structure factor for 60%. Therefore, when the volume fraction is $\phi \approx 0.60$, the effective refractive index of the supraballs is $n_{SB} = 1.331$, according to Equation (1) with $n_{HS} \approx 1.3306$; this explains why the supraballs become transparent in water while they are visible in air or other solvents, as shown in the optical microscopic images in Figure S3, Supporting Information.

Due to intraparticle and interparticle resonant scattering of hollow nanospheres in our supraballs, UV light can be reflected selectively from the supraball solution. As shown in **Figure 4**, the reflectance values were measured and compared with the calculated reflection spectra, as described in a previous report.[33] The maximum peak for the supraballs in air is shown at 279 nm, which is close to the calculated peak value of 267 nm (Figure 4a). However, the significant reflectance (>30%) was observed in the visible light because of multiple scattering from the supraballs with an effective refractive index of 1.331, which was not taken into account in the single scattering calculation. In the photograph shown in Figure 4, the supraballs in air showed white color. By contrast, visible reflectance from supraballs in water was remarkably suppressed because the effective refractive index of supraballs matched the refractive index of water. Notably, our supraballs in water also showed a strong reflection in the
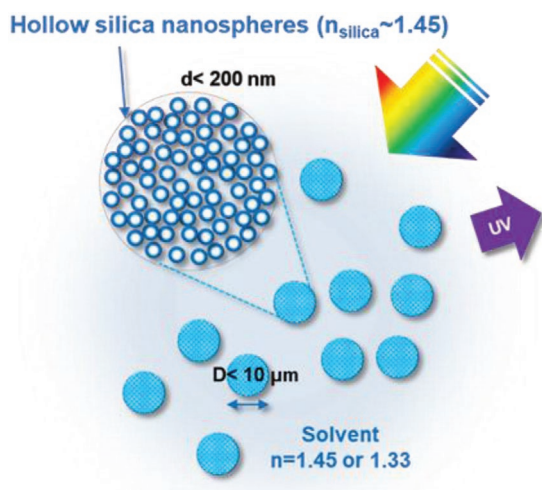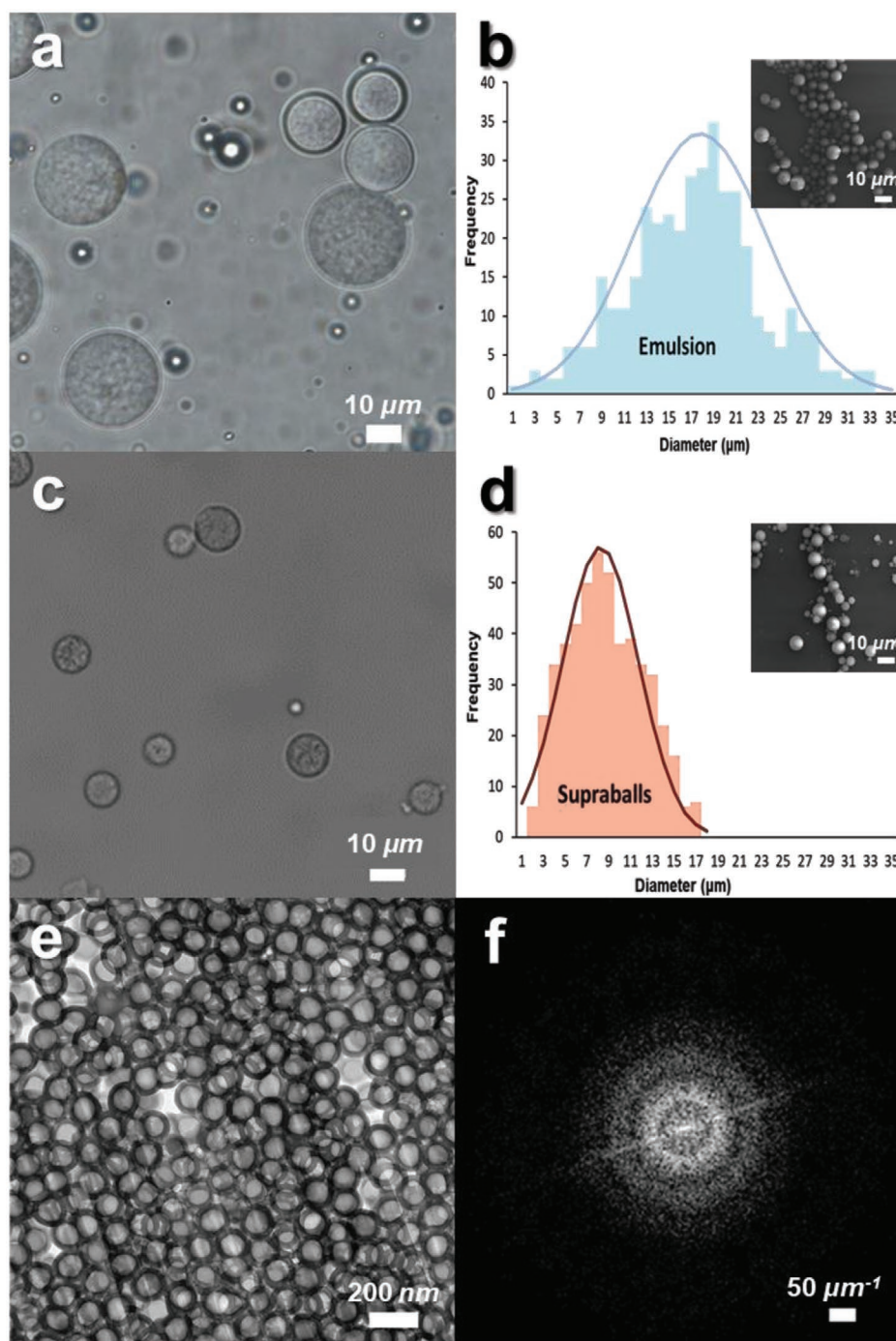
Figure 3. Optical microscopic images and size distribution of a,b) encapsulated hydrophobic PS-VTMS core-shell nanoparticles and c,d) aggregates composed of hollow silica nanoparticles. e) Cross sectional TEM image of a supraball. f) Fast Fourier-transformed (FFT) image of supraball.

UV range, where the peak position shifted to a slightly longer wavelength (≈307 nm) due to the slightly higher average refractive index. The reflection peak shown in Figure 4a was slightly broader than the calculated one, which may be ascribed to the polydispersity of supraballs. According to FEM simulation on light scattering of supraballs with various diameters, as shown in Figure S4, Supporting Information, larger supraballs may have a stronger backscattering and a broader half-maximum full width.

Since water is volatile, it would be practically important to use a nonvolatile solvent, such as ethylene glycol, for transparent UV-reflective supraballs. To this end, we increased the effective refractive index of hollow silica particles by adjusting the core diameter and shell thickness to match the refractive index of the mixture of 60% ethylene glycol and 40% water ($n \approx 1.4$). As shown in Figure S5, Supporting Information, large hollow nanospheres with core diameter of 66 nm and shell thickness of
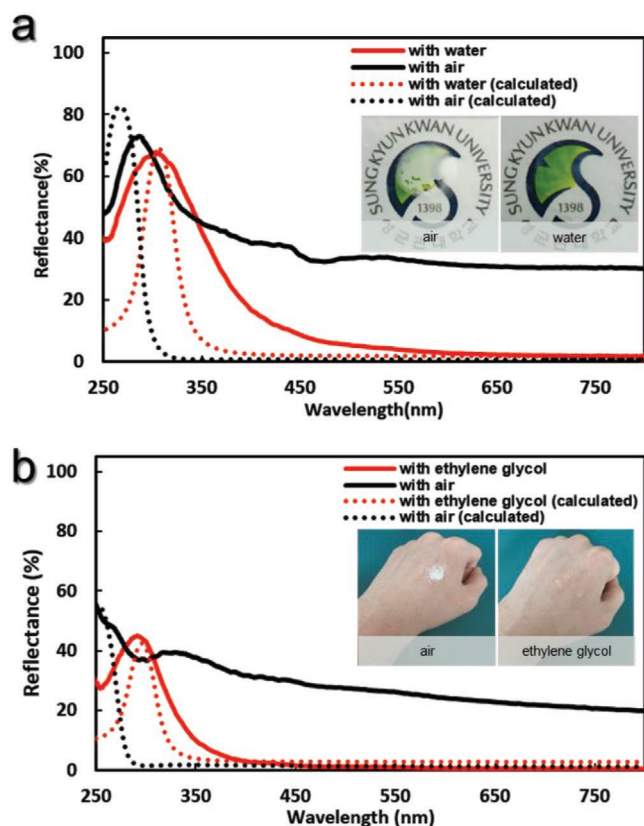
**ADVANCED
SCIENCE NEWS**
www.advancedsciencenews.com

Particle
& Particle Systems Characterization
www.particle-journal.com

Figure 4. Reflectance spectra of supraballs in a) air and water and b) air and ethylene glycol compared with simulation result.

32 nm were successfully prepared by sol–gel reaction of VTMS on polystyrene beads. As shown in Figure 4, these supraballs were white in air due to multiple scattering but became transparent in ethylene glycol. As shown in Figure 4b, the reflection peaks of supraballs in air and ethylene glycol are well matched with the calculation results based on the single scattering theory.

In summary, optically transparent, UV-reflective photonic composite films were prepared by a drop-casting and heat pressing procedure. More specifically, hollow silica nanospheres dispersed in solvent were mixed with the PVDF-HFP polymer, and dropped on the glass substrate and dried at 120 °C. Those photonic films represent highly transparent and UV-reflective properties. Moreover, photonic supraballs with amorphous structures of hollow silica nanospheres were prepared by emulsion encapsulation and shrinkage. Hydrophobic PS-silica core-shell particles were dispersed in an oil in water emulsion in the presence of a surfactant, and supraballs of hollow silica nanosphere were prepared through thermal annealing at 600 °C. While the photonic supraball film in air showed a strong UV reflectance, it also showed a white color due to multiple scattering from supraballs. We mitigated this problem by matching the average refractive index of supraballs with the refractive index of the solvent. Photonic supraballs comprising 140 nm hollow silica nanospheres with 23 nm shell became transparent in water. Moreover, supraballs made of 130 nm hollow silica nanospheres with 32 nm shell became transparent in the mixture of ethylene glycol and water. The photonic films and supraballs prepared in this study should be useful for developing sun protection creams in cosmetic products, functional paints, or UV protective coating on glass for building windows or car windshields. Furthermore, our work can be tuned for another wavelength region, such as IR or visible region, so that sunlight or light in display devices can be utilized more efficiently.

Experimental Section

Materials: Styrene (≥99%, Aldrich), sodium styrene sulfonate (≥90%, NaSS, Aldrich), sodium hydrogen carbonate (NaHCO$_3$, Junsei), potassium persulfate (≥95%, K$_2$S$_2$O$_8$, Junsei), divinylbenzene (80%, DVB, Aldrich), VTMS (>98%, Evonik), ammonium hydroxide solution (NH$_3$·H$_2$O, 28–30%, Merck), TMPEOTA (SK CYTEC), photoinitiator (Darocur 1173, SK CYTEC), poly(vinylidene fluoride-co-hexafluoropropylene) (average $M_n \approx$ 130000, PVDF-HFP, Aldrich), DMAc (≥99.5%, Samchun), trimethoxy(octadecyl)silane (90%, OTMOS, Aldrich), chloroform (>99.5%, Aldrich), poly(ethylene glycol)-*block*-poly(propylene glycol)-*block*-poly(ethylene glycol) (average $M_n \approx$ 14600, F108, Aldrich), toluene (99.8%, Samchun).

Synthesis of PS-VTMS Core-Shell Particles: VTMS (3 mL) in DI water (90 mL) was hydrolyzed under vigorous stirring for 30 min. Simultaneously, 30 mL of PS particle suspension (0.5 wt% PS spheres in water) and ammonium hydroxide solution (28–30 wt%, 8 mL) were mixed in a round-bottom flask for 5 min. The hydrolyzed VTMS solution was added to the PS particle suspension at room temperature. After 12 h stirring, unreacted precursors, ammonia and water were removed by repeated centrifugation using ethanol. For the preparation of core-shell particles with hydrophobic surface, 1.875 mL of chloroform and 0.375 mL of trimethoxy(octadecyl) silane were mixed at 400 rpm for 1 h. Then, absolute ethanol (5.25 mL), ammonium hydroxide solution (1.25 mL), and 10 mL of PS-VTMS particles suspension (10 wt% core-shell particles in ethanol) were mixed. The solution including silane coupling agent was added to the core-shell particles suspension under vigorous stirring. After 4 h, the surface-modified PS-VTMS core-shell particles were washed three times with ethanol.

Preparation of TMPEOTA Composite Films: Hollow silica nanospheres in ethanol were dropped on the glass substrate and dried at 80 °C, which were infiltrated with 100 µL TMPEOTA and a photoinitiator (Darocur 1173) mixture. Then, the TMPEOTA was polymerized under UV irradiation for 5 min.

Preparation of PVDF-HFP Composite Films: For 30 wt% silica–polymer composite film, the powder of hollow silica nanospheres (0.053 g) was dispersed in the 3.5 g of DMAc by ultra-sonication for 1 h and the 0.175 g of PVDF-HFP was mixed by mechanical stirring. Then, the 0.3 mL of DMAc solution of PVDF-HFP and hollow silica nanospheres was dropped on the glass substrate and dried at 120 °C for 30 min. Finally, the composite films were peeled off from the glass substrate carefully, and then annealed at 180 °C under 40 MPa for 10 min. For 40 or 50 wt% composite film, amount of hollow silica nanospheres was increased to 0.07 and 0.088 g, respectively.

Synthesis of Photonic Supraballs: Photonic supraballs of PS-VTMS core-shell particles were produced by oil in water emulsion. First, 0.5 mL of dispersion (10 wt% hydrophobic PS-VTMS core-shell particles in toluene) and 10 mL of continuous phase solution (2 wt% emulsion stabilizer, Pluronic F108) were mixed with a homogenizer in four steps for 1 min. To remove toluene quickly, this solution was heated at 60 °C for 24 h. After the complete reaction, the samples were washed in ethanol by centrifugation and ultra-sonication, and were then annealed at 600 °C to burn out the PS particles and for densification.

Characterization and Measurements: The morphology of the particles and supraballs were observed and analyzed using SEM (Hitachi, S-4300) and TEM (JEOL/CEOS, JEM-2100F) instruments. The cross section of photonic supraballs was prepared using a focused ion beam machine (FIB, SII, SMI3050TB). We measured the UV–vis reflective spectra of photonic supraballs by using a fiber-coupled spectrometer

ADVANCED
SCIENCE NEWS
www.advancedsciencenews.com

Particle
& Particle Systems Characterization
www.particle-journal.com

(Ocean Optics Inc., BH-2000-BAL) equipped with a reflection-mode optical microscope (Nikon, Eclipse 80i). Informed and signed consent was obtained for all experiments involving human volunteers.

Supporting Information

Supporting Information is available from the Wiley Online Library or from the author.

Acknowledgements

Conflict of Interest

The authors declare no conflict of interest.

Keywords

[1] Y. Matsumura, H. N. Ananthaswamy, *Toxicol. Appl. Pharmacol.* **2004**, *195*, 298.
[2] A. L. Andrady, H. S. Hamid, A. Torikai, *Photochem. Photobiol. Sci.* **2003**, *2*, 68.
[3] Y. W. Wang, Z. I. Mo, C. Zhang, P. Zhang, R. B. Guo, H. Gou, R. Hu, X. J. Wei, *J. Ind. Eng. Chem.* **2015**, *32*, 172.
[4] J. R. C. Smirnov, M. E. Calvo, H. Miguez, *Adv. Funct. Mater.* **2013**, *23*, 2805.
[5] Y. Wang, J. Su, T. Li, P. Ma, H. Bai, Y. Xie, M. Chen, W. Dong, *ACS Appl. Mater. Interfaces* **2017**, *9*, 36281.
[6] H. Yin, P. S. Casey, *Mater. Lett.* **2014**, *121*, 8.
[7] J. R. C. Smirnov, M. Ito, M. E. Calvo, C. Lopez-Lopez, A. Jimenez-Solano, J. F. Galisteo-Lopez, P. Zavala-Rivera, K. Tanaka, E. Sivaniah, H. Miguez, *Adv. Opt. Mater.* **2015**, *3*, 1633.
[8] L. Shi, Y. Zhang, B. Dong, T. Zhan, X. Liu, J. Zi, *Adv. Mater.* **2013**, *25*, 5314.
[9] Y. Takeoka, *J. Mater. Chem.* **2012**, *22*, 23299.
[10] P. D. Garcia, R. Sapienza, A. Blanco, C. Lopez, *Adv. Mater.* **2007**, *19*, 2597.
[11] Y. Takeoka, M. Honda, T. Seki, M. Ishii, H. Nakamura, *ACS Appl. Mater. Interfaces* **2009**, *1*, 982.
[12] Y. Takeoka, S. Yoshioka, A. Takano, S. Arai, K. Nueangnoraj, H. Nishihara, M. Teshima, Y. Ohtsuka, T. Seki, *Angew. Chem.* **2013**, *125*, 7402.
[13] J.-G. Park, S.-H. Kim, S. Magkiriadou, T. M. Choi, Y.-S. Kim, V. N. Manoharan, *Angew. Chem., Int. Ed.* **2014**, *53*, 2899.
[14] K. Ueno, A. Inaba, Y. Sano, M. Kondoh, M. Watanabe, *Chem. Commun.* **2009**, *24*, 3603.
[15] A. Kawamura, M. Kohri, G. Morimoto, Y. Nannichi, T. Taniguchi, K. Kishikawa, *Sci. Rep.* **2016**, *6*, 33984.
[16] X. He, Y. Thomann, R. J. Leyrer, J. Rieger, *Polym. Bull.* **2006**, *57*, 785.
[17] S.-H. Kim, S. Magkiriadou, D. K. Rhee, D. S. Lee, P. J. Yoo, V. N. Manoharan, G.-R. Yi, *ACS Appl. Mater. Interfaces* **2017**, *9*, 24155.
[18] S. Magkiriadou, J.-G. Park, Y.-S. Kim, V. N. Manoharan, *Opt. Mater. Express* **2012**, *2*, 1343.
[19] T. J. Freegard, *Eye* **1997**, *11*, 465.
[20] A. Perro, G. Meng, J. Fung, V. N. Manoharan, *Langmuir* **2009**, *25*, 11295.
[21] A. Dang, S. Ojha, C. M. Hui, C. Mahoney, K. Matyjaszewski, M. R. Bockstaller, *Langmuir* **2014**, *30*, 14434.
[22] H. Sabouri, Y. Huang, K. Ohno, S. Perrier, *Nanoscale* **2015**, *7*, 19036.
[23] T.-S. Deng, F. Marlow, *Chem. Mater.* **2012**, *24*, 536.
[24] T. M. Choi, J.-G. Park, Y.-S. Kim, V. N. Manoharan, S.-H. Kim, *Chem. Mater.* **2015**, *27*, 1014.
[25] D. J. Norris, E. G. Arlinghaus, L. Meng, R. Heiny, L. E. Scriven, *Adv. Mater.* **2004**, *16*, 1393.
[26] Y. Takeoka, S. Yoshioka, M. Teshima, A. Takano, M. Harun-Ur-Rashid, T. Seki, *Sci. Rep.* **2013**, *3*, 2371.
[27] Y.-S. Cho, S.-H. Kim, G.-R. Yi, S.-M. Yang, *Colloids Surf. A* **2009**, *345*, 237.
[28] M. Xiao, Z. Hu, Z. Wang, Y. Li, A. D. Tormo, N. L. Thomas, B. Wang, N. C. Gianneschi, M. D. Shawkey, A. Dhinojwala, *Sci. Adv.* **2017**, *3*, e1701151.
[29] Y. Zhao, L. Shang, Y. Cheng, Z. Gu, *Acc. Chem. Res.* **2014**, *47*, 3632.
[30] N. Vogel, S. Utech, G. T. England, T. Shirman, K. R. Phillips, N. Koay, I. B. Burgess, M. Kolle, D. A. Weitz, J. Aizenberg, *Proc. Natl. Acad. Sci. USA* **2015**, *112*, 10845.
[31] S. G. Romanov, S. Orlov, D. Ploss, C. K. Weiss, N. Vogel, U. Peschel, *Sci. Rep.* **2016**, *6*, 27264.
[32] K. W. Desmond, E. R. Weeks, *Phys. Rev. E* **2014**, *90*, 022204.
[33] S. Magkiriadou, J.-G. Park, Y.-S. Kim, V. N. Manoharan, *Phys. Rev. E* **2014**, *90*, 062302.